THE SOUTHERN GALACTIC PLANE SURVEY: NEW VIEWS OF THE DEEP SOUTH

Bryan M. Gaensler[1], **Naomi M. McClure-Griffiths**[2], **John M. Dickey**[3], **Anne J. Green**[4]

[1] ***Harvard-Smithsonian Center for Astrophysics, 60 Garden Street MS-6, Cambridge, MA 02138, USA.***
e-mail: bgaensler@cfa.harvard.edu

[2] ***Australia Telescope National Facility, CSIRO, PO Box 76, Epping, NSW 1710, Australia.***
e-mail: Naomi.McClure-Griffiths@csiro.au

[3] ***Department of Astronomy, University of Minnesota, 116 Church Street SE, Minneapolis, MN 55455, USA.***
e-mail: john@astro.umn.edu

[4] ***Astrophysics Department, School of Physics, University of Sydney, NSW 2006, Australia.***
e-mail: agreen@physics.usyd.edu.au

ABSTRACT

The Southern Galactic Plane Survey (SGPS) is an effort to map the southern Galaxy in the HI line and in 1.4-GHz polarized continuum emission. These data consist of 2200 mosaiced pointings obtained with the Australia Telescope Compact Array, combined with lower resolution observations taken with the multibeam receiver of the Parkes Radio Telescope. I will describe the analysis procedures associated with the polarized continuum emission, show the resulting images, and explain how these data are a powerful probe of the turbulence and large-scale structure of magneto-ionic gas in the interstellar medium.

INTRODUCTION

Radio emission in the plane of the Milky Way shows significant levels of linear polarization. There are two sources of this polarization: discrete objects such as supernova remnants (SNRs), and a diffuse polarized background produced by the relativistic component of the interstellar medium (ISM). All of this emission undergoes Faraday rotation as it propagates towards us, either in the source itself or in intervening material. With sufficiently high angular and frequency resolution, we can use the properties of this polarized emission to map out the distribution of ionized gas and magnetic fields in individual sources and in the ambient ISM. However, only recently have detailed studies of this effect been carried out.

Here we describe our efforts to make polarimetric images of the entire fourth quadrant of the Galaxy with the Australia Telescope Compact Array (ATCA). These data have been taken as part of the Southern Galactic Plane Survey (SGPS; [1]). While the primary focus of the SGPS is to study the Galactic distribution of H I, the ATCA simultaneously receives full polarimetric continuum data, which have allowed us to map out the distribution of linearly polarized emission in the survey region. We briefly summarize a few aspects of this work here; our analysis is described in more detail in [2].

OBSERVATIONS AND ANALYSIS

The ATCA is a 6-element synthesis telescope, located near Narrabri, NSW, Australia. Observations for the SGPS were carried out in the period 1998 December to 2000 August, and consisted of 2200 mosaiced pointings covering the region $253^\circ < l < 358^\circ$ and $-1^\circ < b < +1^\circ$ (see [3] for details). Data. were recorded in nine spectral channels spread across 96 MHz of bandwidth and centered at a frequency of 1384 MHz. A set of nearby unresolved background sources were each observed over a wide range in parallactic angle in order to solve for the instrumental polarization characteristics of each antenna [4]. The calibrated data were then converted to the four standard Stokes parameters, I, Q, U and V.

For each spectral channel and each pointing, the visibilities were then inverted to produce an image, employing a uniform weighting scheme to minimize sidelobe contributions from strong sources. A mosaiced image of each sub-region was formed for each of the nine spectral channels and four Stokes parameters by linearly combining the data from the 105 separate pointings [5, 6]. The four Stokes images for each spectral channel were deconvolved jointly using the maximum entropy algorithm PMOSMEM [7]. This approach successfully recovers the large-scale structure measured by the mosaicing process [8], and also uses the "maximum emptiness" criterion, which allows the Stokes Q, U and V maps to take on negative values. No constraints were given to the deconvolution process regarding the total flux density in each image or sub-region to be deconvolved. Following deconvolution, each image was smoothed with a gaussian restoring beam of appropriate dimensions. Images of linearly polarized intensity, $L = (Q^2 + U^2)^{1/2}$, linearly polarized position

angle, $\Theta = \frac{1}{2}\tan^{-1}(U/Q)$, and uncertainty in position angle, $\Delta\Theta = \sigma_{Q,U}/2L$, were then formed from each pair of Q and U images, where $\sigma_{Q,U}$ is the RMS sensitivity in the Q and U images. A correction was applied to the L images to account for the Ricean bias produced when Q and U are combined. The nine L maps (one per spectral channel) were then averaged together to make a final image of L for each sub-region.

RESULTS

In Fig 1 we show images of I and L for an initial test region for the SGPS, covering 28 deg^2 (see [2] for details). In this figure, we show both our 1.4-GHz ATCA observations and those from the 2.4-GHz Parkes survey of [9] (resolution $10\farcm4$). The total intensity images show the presence of SNRs and H II regions (see [1] for further discussion). Although the interferometric ATCA observations are not sensitive to the diffuse emission seen by Parkes, it is clear that the same features are present in both data-sets.

The ATCA L image reveals two large voids of reduced polarization, each elliptical and several degrees in extent. One void is centered on $(l, b) = (332\fdg4, +1\fdg4)$ ("void 1") and the other on $(328\fdg2, -0\fdg5)$ ("void 2"); both voids are also seen in the 2.4-GHz Parkes polarization map. The rotation measures (RMs) around the edges of these voids range up to ± 400 rad m^{-2}, in distinction to the low RMs seen over the rest of the field.

DISCUSSION

We first note that the incomplete $u - v$ coverage of an interferometer affects images of polarization in complicated ways. While it is physically required that $L \leq I$, and we generally expect that structures seen in L might correspond to similar structures in I, neither situation will be generally observed in interferometric data. This is because an interferometer can not detect structures larger than a certain size, corresponding to the closest spacings between its antenna elements (in the case of the ATCA, this maximum scale is $\sim 35'$). A source larger than this maximum scale will not be seen in Stokes I; if it is also a uniformly polarized source, it will not be detected in polarization either. However, magnetic field structure within the source, plus variations in the Faraday rotation along different lines-of-sight, can introduce power in Stokes Q and U on smaller scales, to which the interferometer is sensitive. We thus can often observe complicated structures in polarization which have no counterpart in total intensity [10, 11, 12]. Clearly such an effect is occurring here, and is producing virtually all the linear polarization seen in Figure 1. We can crudely divide up the diffuse polarization we see into two components.

The brightest polarization seen with the ATCA matches well the bright polarized structures seen with Parkes. Since the amount of Faraday-induced polarization is very strongly dependent on both resolution and frequency, the fact that two such disparate data-sets show similar structures implies that these bright polarized structures are intrinsic to the emitting regions, which are most likely at a distance of ~ 3.5 kpc [2]. The rest of the ATCA field is filled with fainter diffuse polarization, which does not have any counterpart in the Parkes data. This emission is best explained as being due to Faraday rotation in foreground material. The RMs measured for this emission imply that they are caused by foreground clouds of RM ~ 5 rad m^{-2}, consistent with the conclusions made by [10].

To the best of our knowledge, voids in polarization such as those described here have not been previously reported. There are two possible explanations to account for these structures: either they represent regions where the level of intrinsic polarization is low, or they are the result of propagation through a foreground object, whose properties have depolarized the emission at both 1.4 and 2.4 GHz.

If the voids are intrinsic to the emitting regions, then the distance of 3.5 kpc derived in [2] implies that they are hundreds of parsecs across — it is hard to see what could produce such uniformly low polarized intensity across such large regions. We thus think it unlikely that the voids are intrinsic to the emitting regions. We therefore favor the possibility that the voids are caused by depolarizing effects in foreground material. We have considered in detail the various ways in which foreground Faraday rotation can produce the observed structure, and can rule out bandwidth and gradient depolarization as possible mechanisms (see [2] for details).

The only remaining possibility is that depolarization in the voids is due to beam depolarization, in which the RM varies randomly on small scales. We have developed a detailed model for "void 1" to confirm this. We consider void 1 to be a caused by a sphere of uniform electron density n_e cm^{-3}, centered on $(332\fdg5, +1\fdg2)$ with a radius of $1\fdg4$ and at a distance to us of d kpc. Within the sphere, we suppose that there are random and ordered components to the magnetic field, and that these two components have identical amplitudes B μG. The ordered component is uniformly oriented at an angle θ to the line of sight. We assume that the random component is coherent within individual cells of size l pc, but that the orientation from cell to cell is random. Uniformly polarized rays which propagate through a different series of cells will

experience differing levels of Faraday rotation, resulting in beam depolarization when averaged over many different paths.

By calculating the properties of the polarized signal which emerges after propagating through this source, we find that we can account for the observed properties of void 1 if $n_e \sim 20$ cm^{-3}, $B \sim 5$ μG, $\theta \gtrsim 80^\circ$, $d \sim 300$ pc and $l \sim 0.2$ pc (see [2] for details). These properties are consistent with those of an H II region of comparatively low emission measure. It is interesting to note that the O9V star HD 144695 is very close to the projected center of void 1, and is at a distance of 300 ± 160 pc. The radius of the Strömgren sphere which this star would produce is consistent with the extent of the void. It is thus reasonable to propose that the star is embedded in and powers the surrounding ionized bubble.

Two properties of the voids which our simple model cannot account for are the requirement that the uniform component of the magnetic field be largely oriented in the plane of the sky, but that we generally observe coherent regions of large RM (of the order of a few hundred rad m^{-2}) around the edges of the voids. We suggest that both these results can be explained by the field geometry which arises during the expansion phase of an H II region as it interacts with surrounding material. This produces a magnetic field perpendicular to the line of sight over most of the void, but which is parallel to the line of sight (and can thus potentially produce high RMs) around the perimeter.

SUMMARY

The ATCA's sensitivity, spatial resolution and spectral flexibility allow us to study linear polarization and Faraday rotation from the inner Galaxy in an unprecedented detail. Using our SGPS data, we have been able to identify a variety of distinct polarimetric phenomena, and have used these to map out both global and turbulent structures in the magneto-ionized ISM. We anticipate that our analysis will ultimately result in a comprehensive study of magnetic fields and turbulence in the inner Galaxy.

ACKNOWLEDGMENTS

The Australia Telescope is funded by the Commonwealth of Australia for operation as a National Facility managed by CSIRO. Support for the SGPS survey has been provided by National Science Foundation grant AST-9732695 to the University of Minnesota.

REFERENCES

[1] McClure-Griffiths, N. M., Green, A. J., Dickey, J. M., Gaensler, B. M., Green, A. J., Haynes, R. F., and Wieringa, M. H., *The Astrophysical Journal*, **551**, 394–412 (2001).

[2] Gaensler, B. M., Dickey, J. M., McClure-Griffiths, N. M., Green, A. J., Wieringa, M. H., and Haynes, R. F., *The Astrophysical Journal*, **549**, 959–978 (2001).

[3] McClure-Griffiths, N. M., PhD Thesis, University of Minnesota (2001).

[4] Sault, R. J., Hamaker, J. P., and Bregman, J. D., *Astronomy & Astrophysics Supplemental Series*, **117**, 149–159 (1996).

[5] Cornwell, T. J., Holdaway, M. A., and Uson, J. M., *Astronomy & Astrophysics*, **271**, 697–713 (1993).

[6] Sault, R. J., Staveley-Smith, L., and Brouw, W. N., *Astronomy & Astrophysics Supplemental Series* , **120**, 375–384 (1996).

[7] Sault, R. J., Bock, D. C.-J., and Duncan, A. R., *Astronomy & Astrophysics Supplemental Series*, **139**, 387–392 (1999).

[8] Ekers, R. D., and Rots, A. H., in *Image Formation from Coherence Functions in Astronomy*, edited by C. van Schooneveld, Reidel, Dordrecht, pp. 61–63 (1979).

[9] Duncan, A. R., Haynes, R. F., Jones, K. L., and Stewart, R. T., *Monthly Notices of the Royal Astronomical Society*, **291**, 279–295 (1997).

[10] Wieringa, M. H., de Bruyn, A. G., Jansen, D., Brouw, W. N., and Katgert, P., *Astronomy & Astrophysics*, **268**, 215–229 (1993).

[11] Haverkorn, M., Katgert, P., and de Bruyn, A. G., *Astronomy & Astrophysics*, **356**, L13–L15 (2000).

[12] Gray, A. D., Landecker, T. L., Dewdney, P. E., and Taylor, A. R., *Nature*, **393**, 660–662 (1998).

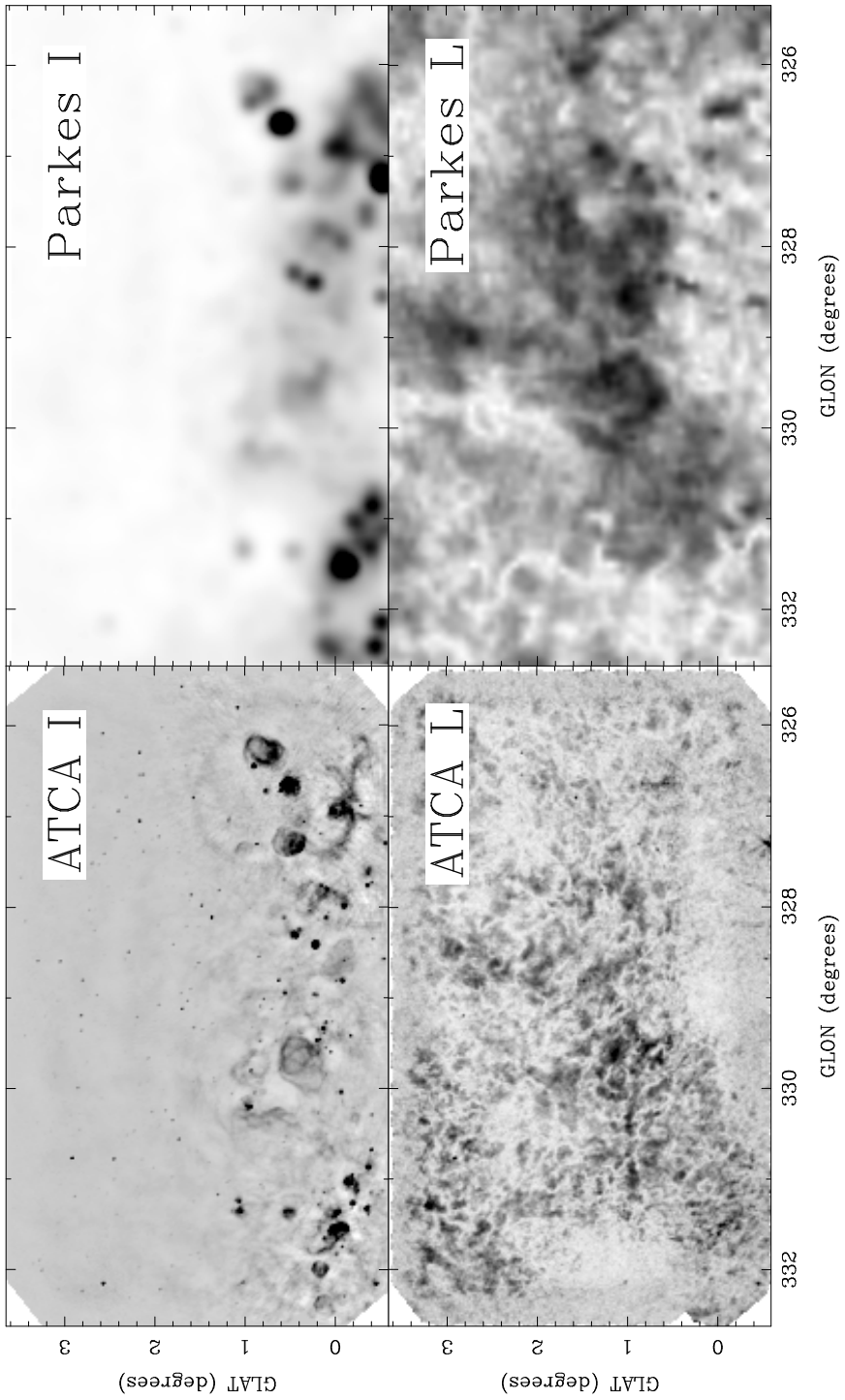

Figure 1: Images of the SGPS test region made with the ATCA (1.4 GHz, 1 arcmin resolution) and Parkes (2.4 GHz, 10.4 arcmin), in both total (I) and linearly polarized (L) intensity.